IPPI
Polyolefins Journal, Vol. 3 No. 1 (2016) 1-9
ORIGINAl PAPER

Influence of annealing on anisotropic crystalline structure of HDPE cast films

Ali Yadegari[1,2], Jalil Morshedian[1*], Hossein-Ali Khonakdar[1,2], Udo Wagenknecht[2]

[1] Faculty of Processing, Iran Polymer and Petrochemical Institute, P.O. Box 14975/112, Tehran, Iran
[2] Leibniz-Institut für Polymerforschung Dresden e. V., Hohe Str. 6, D-01069 Dresden, Germany

Received: 10 May 2015, Accepted: 7 September 2015

ABSTRACT

High density polyethylene (HDPE) films were produced using cast film extrusion process with different draw ratios, ranging from 16.9 to 148.8. Morphology, crystallinty and orientation state of crystalline and amorphous phases of the cast films were investigated using scanning electron microscopy (SEM), differential scanning calorimetry (DSC) and polarized Fourier transform infrared spectroscopy (FTIR) analyses, respectively. The anisotropic crystalline structures of row-nucleated lamellar morphology were observed for the films produced with high draw ratios. The crystalline phase axes orientation functions were found to be significantly dependent on the applied draw ratios. As expected, annealing increased the crystallinity and melting point temperature (T_m) of the cast films and on the other hand, it also enhanced the crystalline phase orientation. However, the results revealed that annealing also promoted non-twisted lamellar structures, since it increased the f_c values (*c*-axis orientation function) and decreased the f_a values (*a*-axis orientation function) simultaneously. Additionally, it was found that the annealing induced enhancement in *c*-axis orientation function was more significant for the cast films with lower draw ratios, therefore, it was dependent on the draw ratio. **Polyolefins J 3:1-9**

Keywords: HDPE; cast film extrusion; crystal orientation; annealing; crystallinity

INTRODUCTION

Processing of semi-crystalline polymeric materials using important industrial technologies such as extrusion, imposes different levels of flow fields to the polymer melt [1,2]. These flow fields which are elongation or shear, bring different degrees of anisotropy in the polymer melt, and ultimately, change the rate of solidification, the semi-crystalline morphology and material properties [3, 4].

It is known that the crystallization behavior of semi-crystalline polymers is significantly determined by the process conditions [3,5]. The spherulitic structure is formed in low stresses or a quiescent state and leads to the arrangement of crystal blocks or lamellae in a spherical shape resulting in an isotropic configuration. Besides, the row-nucleated lamellar structure is developed when the polymer is crystallized under high or moderate stresses [2,6].

In cast film extrusion followed by stretching, polymers having high degree of crystallinity experience elongation stress and then they are recrystallized, which is called as stress induced crystallization and finally a lamellar crystalline structure can be formed [7,8]. The orientation of polymer chains and the large

* Corresponding Author - E-mail: J.Morshedian@ippi.ac.ir

scale lamellar morphology are identified as two key factors in determining the performance and behavior of final produced films. Therefore, a great deal of effort has been undertaken to explain the relationship between the processing conditions and the structure and properties of extruded films [9-12].

On the other hand, annealing of semi-crystalline polymers at high temperatures between glass transition temperature (T_g) and melting temperature (T_m) is observed to be an effective procedure to encourage chain relaxation toward a thermodynamically more stable state and induce remarkable variations in microstructure and physical properties [13-15]. An important requirement allowing crystal perfection and thickening is the occurrence of chain axis crystalline mobility. The thermal transition ascribed to this is generally represented as the α_c relaxation [16,17]. The α_c relaxation is attributed to the activation of molecular motions in the crystalline phase. The association between the average crystallite thickness and temperature of the α_c peak in a dynamic mechanical analysis is a demonstration of thermal activation of the migration of defects in the crystalline phase [18].

Throughout the annealing procedure, the lamellar thickness increases and the lamellar orientation and uniformity are improved in the cast films with row-nucleated lamellar structure, companied with the eliminating of the defects in the crystalline structure [19,20].

The relationship between annealing treatment and properties of semi-crystalline polymers, such as elastic recovery of HDPE cast films [7], toughening of β-form polypropylene [15], microstructure and mechanical properties of polypropylene with β-phase nucleating agent [21], deformation mechanism of polypropylene films [19], and porosity enhancement in polypropylene stretched films [22] has been investigated.

Polyethylene is one of the most used thermoplastic commodities since it has good mechanical properties, chemical resistance and processability [23,24]. Furthermore, polyethylene films are considered as precursors for microporous membranes production by dry-stretching [10,25]. In this study, the role of applying a wide range of draw ratios (from 16.9 to 148.8) and the annealing on lamellar crystalline orientation and the degree of crystallinity in HDPE cast films are examined. In addition, the development of oriented structure of three crystalline phase axes on annealing is studied with FTIR spectroscopy. Furthermore, to our knowledge no work has been published regarding the effectiveness of annealing on lamellar orientation improvement as a function of applied draw ratio in the HDPE cast films. It will be shown that draw ratio has a significant role on the *c*-axis orientation function improvement upon annealing, which is the first attempt to address this issue.

EXPERIMENTAL

Material

A commercial HDPE resin (HDPE HTA 108) supplied by ExxonMobil Chemical Company was employed in this study. Its melt index (190 °C/2.16 kg) was 0.70 g/10 min (under ASTM D 1238 conditions provided by company). The molecular weight (M_w) and polydispersity index (*PDI*) of the resin were measured using a PL-GPC 220 with 1,2,4-trichlorobenzene as a solvent and a column temperature of 150 °C, and their values were 111 kg/mol and 6.6, respectively. The melting point temperature (T_m) and the crystallization temperature (T_c) of the resin obtained from differential scanning calorimetry (DSC Q2000) at a rate of 10 °C/min, were 133 °C and 118 °C, respectively.

Film preparation

The cast films were manufactured using a single screw extruder operating at 40 rpm. Temperatures of extruder barrel and slit die were set to 200 °C. The exit cross section, $w_i \times t_i$, of the slit die was set to 250×0.5 mm^2 and 250×1.4 mm^2 in two different extrusion processes. The temperature of the chill rolls was set at 100°C. The rotation velocity of the chill rolls was varied, and the draw ratio (DR) was determined as the ratio of initial ($w_i \times t_i$) and final ($w_f \times t_f$) cross sections of the cast films [12,26]. Thickness, width and applied draw ratios of the cast films are listed in Table 1.

Afterwards, the HDPE cast films were annealed in a fan-assisted oven at a temperature of 120°C for 120 min. For convenience, they were denoted as a code of An-DR x, where x indicates the applied draw ratio.

Characterization

Polarized Fourier transform infrared spectroscopy (FTIR)

The Vertex 80v FTIR vacuum spectrometer equipped with a DLaTGS detector (Bruker, Germany) was used;

Table 1. Applied draw ratios for the preparation of the cast films.

sample	w_f (mm)	t_f (mm)	DR=(w_i×t_i)/(w_f×t_f)
slit die cross section (w_i×t_i): 250×0.5 mm²			
DR 16.9	205	0.036	16.9
DR 25.5	204	0.024	25.5
DR 52.1	200	0.012	52.1
slit die cross section (w_i×t_i): 250×1.4 mm²			
DR 93	198	0.019	93
DR 119	196	0.015	119
DR 148.8	196	0.012	148.8

spectra were measured in vacuum. The IR radiation was polarized by a wire-grid polarizer alternately parallel and perpendicular to the drawing direction using additionally computer-controlled motorized rotational unit for polarizers (Bruker, Germany). The used spectroscopic range was 4000-400 cm^{-1}. The spectral resolution was 2 cm^{-1} and 32 scans were co-added for each spectrum. If the films are oriented, the absorption of plane-polarized radiation by a vibration in two orthogonal directions, specifically parallel and perpendicular to a reference axis, i.e. machine direction (MD), should be different. The ratio of these two absorbance values is defined as the dichroic ratio, *D* [27, 28]:

$$D = \frac{A_{\parallel}}{A_{\perp}} \quad (1)$$

where, $A_{||}$ is the absorbance parallel and $A_{\perp}$ is the absorbance perpendicular to a specific reference axis. The Herman's orientation function of a particular absorbance band vibration is obtained according to [29]:

$$f_i = \frac{(D-1)}{(D+2)} \quad (2)$$

When a crystalline axis is perfectly aligned along the reference axis (machine direction), $f_i = +1$, whereas for the case of perpendicular orientation, $f_i = -1/2$. For random orientation it can be shown that $f_i = 0$ [10]. For polyethylene, absorbance at the wavenumber of 730 cm^{-1} is attributed to the *a*-axis of the unit crystal cell while absorbance at the wavenumber of 720 cm^{-1} is due to the *b*-axis. The orientation function of the *c*-axis is calculated according to the orthogonality equation [27, 28]:

$$f_a + f_b + f_c = 0 \quad (3)$$

An amorphous orientation function, f_{am}, can also be evaluated from dichroism values using the amorphous band at 1368 cm^{-1} [10].

Differential scanning calorimetry (DSC)

The degree of crystallinity, X_c, of the samples was determined from the heat of fusion using a DSC Q2000 at a heating rate of 10 °C/min with a sample weight of about 5.0 mg. The fractional crystallinity (mass fraction) X_c was calculated based on DSC data according to the equation:

$$X_c(\%) = \frac{\Delta H}{\Delta H_0} \times 100 \quad (4)$$

where, ΔH_0 is the specific heat of melting of an ideal crystal. All the reported values were collected from the first heating data. For polyethylene, the commonly accepted value of ΔH_0 = 290 J/g has been used in this study [30].

Scanning electron microscopy (SEM)

The lamellar crystalline morphology of the HDPE cast films was observed using an Ultra Plus Field Emission Gun Scanning Electron Microscope (FEG-SEM, Carl-Zeiss AG, Oberkochen, Germany). The accelerating voltage applied during SEM observation was 3.0 kV.

RESULTS AND DISCUSSION

The lamellar crystalline structure of produced HDPE cast films in different processing conditions, i.e. different draw ratios, were observed using FE-SEM micrographs. Examples of SEM micrographs of the surface of the samples DR 16.9 and DR 148.8 are shown in Figure 1. The micrographs distinctly indicate the importance of applied draw ratio in flow induced crystalline structures. The developed crystalline structure in the sample DR 16.9 is not appeared to be a large superstructure and the spherulitic-like structures are rarely promoted, however, the lamellar growth perpendicular to the MD direction is not completely developed. It is seen that when the high elongation stress was applied, as in the case of sample DR 148.8, the crystalline lamellae tilted toward preferential alignment with respect to stretching direction and the lamellar twisting hardly occurred, resulting in a well-developed stacked lamellar structure. The FE-SEM of sample DR 148.8 presented in the Figure 1 shows the row-nucleated morphology in the form of stacked lamellae obtained via applying high draw ratios. Larger

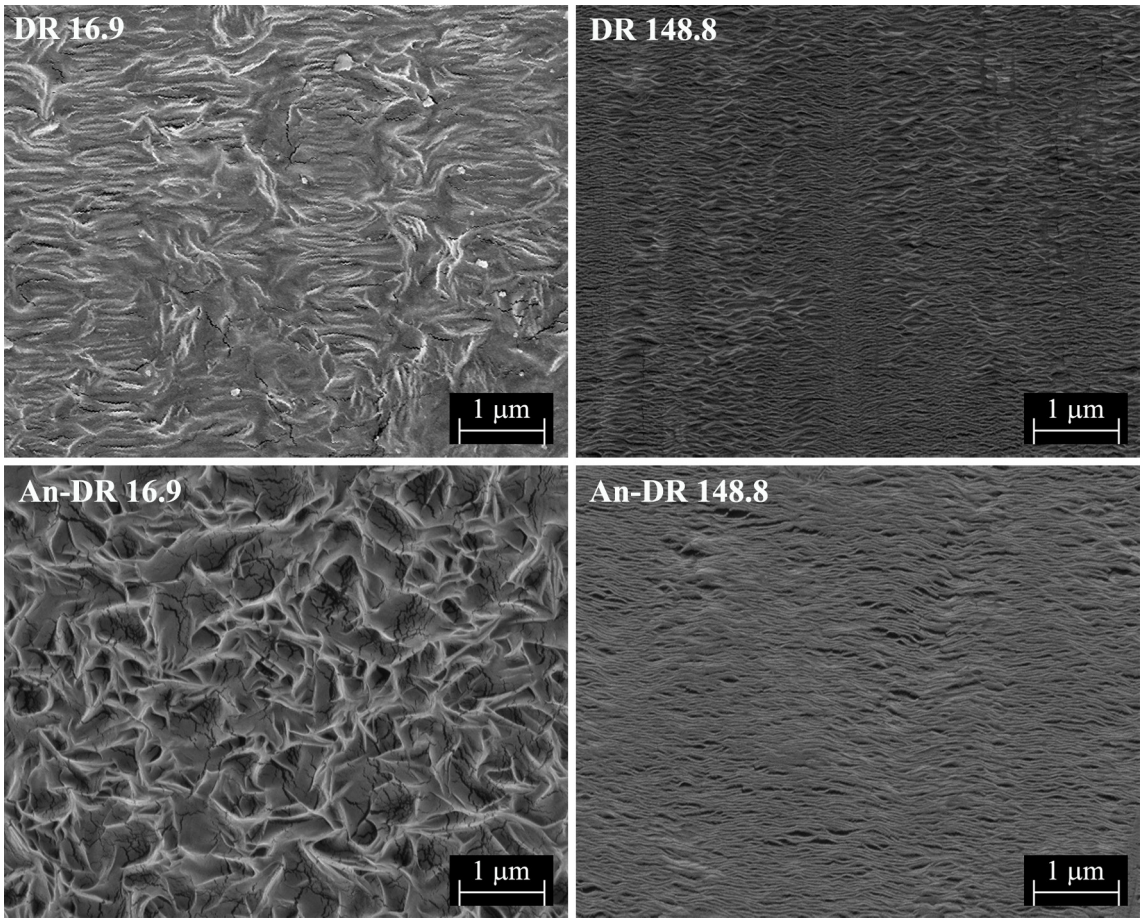

Figure 1. FE-SEM micrographs of HDPE cast films (MD↑, TD→): DR 16.9 and DR 148.8 (before annealing); An-DR 16.9 and An-DR 148.8 (after annealing).

draw ratios will enhance the extension of the chains in the melt state, and preservation of the extended form of the chains for the crystallization before their relaxation will promote the radial growth of the lamellae on the extended chains [31, 32]. Furthermore, the lamellae thickness is decreased and being more uniform with increasing draw ratio. The FE-SEM micrographs of annealed samples of An-DR 16.9 and An-DR 148.8 are also shown in Figure 1. The surface images indicate that annealing leads to lamellar thickening, and more distinctive lamellae are developed.

The effects of applying different draw ratios and annealing on the thermal behavior of the cast films were examined using differential scanning calorimetry (DSC) and the results for the samples DR 16.9 and DR 148.8 are shown in Figure 2. Additionally, melting peak temperatures (T_m) and crystallinity (X_c) of the cast films before and after annealing are listed in Table 2.

The recorded endotherms do not show any significant differences in the positions of the melting peaks of the samples before annealing (black curves in the Figure 2). However, they exhibit different shapes of heating scans, i.e. their height and FWHM (full width at half maximum) values are different. This demonstrates that the distribution of the lamellae thicknesses and their average values are not similar [3]. A single rather sharp melting peak is noticed for the sample DR 148.8. This narrower melting curve without any additional peak or shoulder indicates a more uniform crystal size structure for the films prepared at higher draw ratio conditions. This conclusion also supports the results obtained from SEM micrographs.

The effect of annealing process on the crystalline structure, i.e. the changes of T_m, X_c, peak height and also FWHM of the samples has been investigated and the results are presented in Table 2. It is seen that after annealing, T_m is increased for all the samples. Calculated X_c was also observed to increase, which indicated that compared with the crystal perfectness reflected by increase in the T_m values, the overall degree of crystallinity that was reflected by ΔH, was significantly affected by annealing. Moreover, the microstructural changes as appearance of a shoulder endotherm usu-

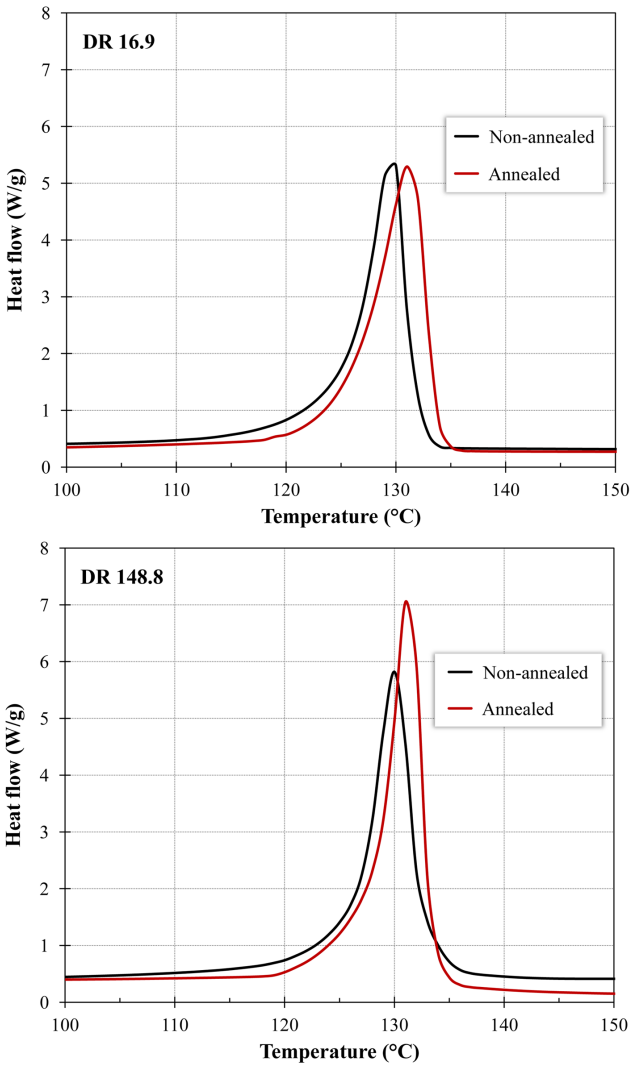

Figure 2. First heating scans of the samples DR 16.9 and DR 148.8 before and after annealing.

ally called an "annealing peak" in DSC thermograms was not observed for the annealed HDPE cast films. It is worth to note when the applied draw ratio increased from 16.9 to 25.5, the peak height was considerably increased, additionally, annealing raised the peak height for the samples with draw ratios higher than 25.5, and it is noticed that after annealing the peak heights were almost in the same range for the samples with higher draw ratios. Eventually, this supports the notion that annealing at elevated temperature is an effective method to promote chain relaxation toward a thermodynamically more stable state [15].

The arrangement and orientation of the crystal lamellae in the HDPE films are among the main elements in controlling the final properties of manufactured films [10]. The orientation of the crystalline phase axes, f_a, f_b and f_c, in addition to the orientation of the amorphous phase, f_{am}, were obtained using FTIR measurements. The FTIR spectra of the samples DR 16.9 and DR 148.8 for the bands at 730 and 720 cm^{-1} and also the band at 1368 cm^{-1} obtained on the annealed and non-annealed films are presented in Figures 3 and 4, respectively. Considering these figures, it is very clear that applying different draw ratios influences remarkably the absorbance intensities of the cast films. Furthermore, annealing also causes significant changes in absorbance intensities which lead to vary the calculated dichroic ratios of the corresponding bands and consequently the orientation functions.

Table 3 collects the orientation functions of the crystalline phase axes as well as of the amorphous phase obtained from FTIR for the HDPE cast films before and after annealing. It can be observed that the *a*-axis orientation function (f_a) tends to decrease when draw ratio increases, and finally it reaches the value of -0.45 for the sample DR 148.8 which shows the *a*-axis arranges itself almost perpendicular to the MD direction when high stress is applied during crystallization of

Table 2. Crystallinities and melting temperatures of cast films before and after annealing.

Before annealing						
	DR 16.9	**DR 25.5**	**DR 52.1**	**DR 93**	**DR 119**	**DR 148.8**
T_m (°C)	129.6	129.8	130.1	130.4	130.3	130.1
X_c (%)	60.4	58.3	59.6	61.7	63.6	61.5
Peak height (W/g)	5.0	5.8	6.1	5.5	6.0	5.4
FWHM (°C)	4.1	3.2	3.4	3.7	3.5	3.7
After annealing						
	An-DR 16.9	**An-DR 25.5**	**An-DR 52.1**	**An-DR 93**	**An-DR 119**	**An-DR 148.8**
T_m (°C)	131.3	131.0	131.2	131.9	131.2	131.3
X_c (%)	65.4	65.5	67.5	67.1	66.0	66.6
Peak height (W/g)	5.0	6.5	6.8	6.5	6.8	6.8
FWHM (°C)	5.0	3.6	3.6	3.8	3.4	3.4

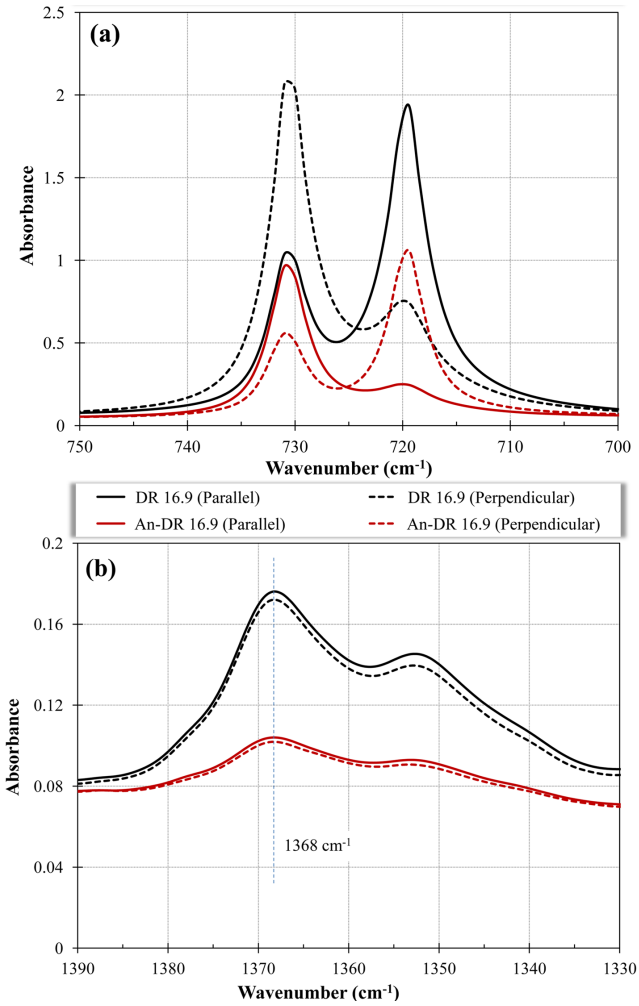

Figure 3. FTIR spectra of the sample DR 16.9 for the bands at 730 and 720 cm^{-1} (a), and band at 1368 cm^{-1} (b); obtained on annealed and non-annealed films.

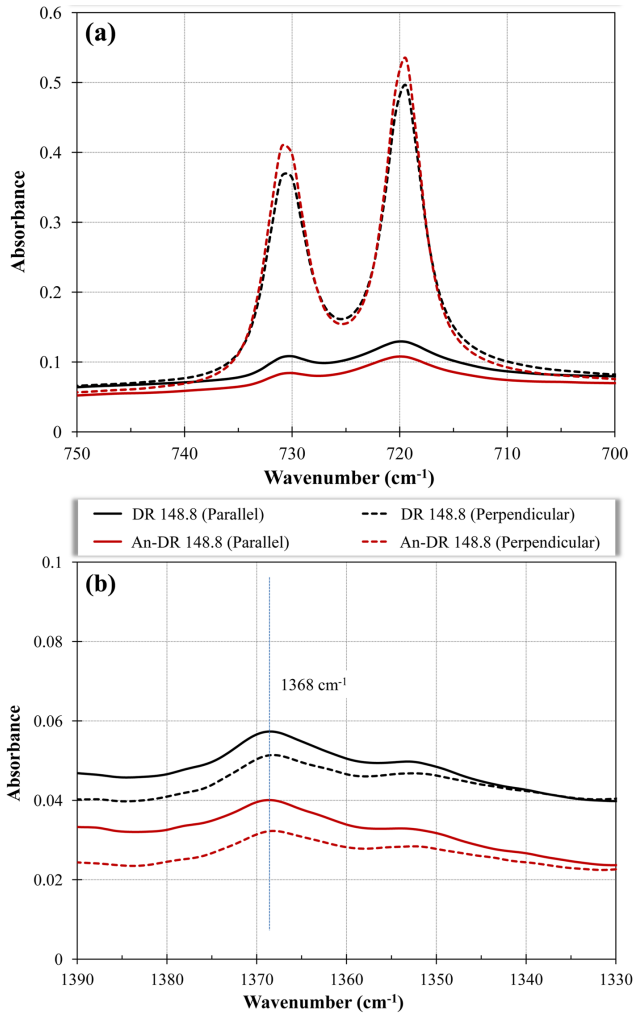

Figure 4. FTIR spectra of the sample DR 148.8 for the bands at 730 and 720 cm^{-1} (a), and band at 1368 cm^{-1} (b); obtained on annealed and non-annealed films.

the cast films. However, it is not the case observed for the f_b values. The *b*-axis orientation functions, f_b, are nearly the same, i.e. around -0.40, for the different draw ratios applied. These values indicate the *b*-axis is more or less laid perpendicular to the MD direction even though high stress is not applied during the film production. The *c*-axis orientation functions (f_c) listed in Table 3 show that their values are increased as a function of draw ratio. Returning to the SEM images in Figure 1 and also regarding orientation functions

Table 3. Calculated orientation functions for the cast films before and after annealing.

Before annealing						
	DR 16.9	**DR 25.5**	**DR 52.1**	**DR 93**	**DR 119**	**DR 148.8**
f_a	0.40	0.22	-0.04	-0.32	-0.42	-0.45
f_b	-0.38	-0.41	-0.41	-0.40	-0.38	-0.38
f_c	-0.02	0.19	0.45	0.72	0.80	0.83
f_{am}	0.00	0.04	0.05	0.08	0.10	0.07
After annealing						
	An-DR 16.9	**An-DR 25.5**	**An-DR 52.1**	**An-DR 93**	**An-DR 119**	**An-DR 148.8**
f_a	0.32	0.12	-0.15	-0.40	-0.43	-0.47
f_b	-0.44	-0.43	-0.43	-0.41	-0.41	-0.41
f_c	0.12	0.31	0.58	0.81	0.84	0.88
f_{am}	0.02	0.03	0.05	0.10	0.08	0.09

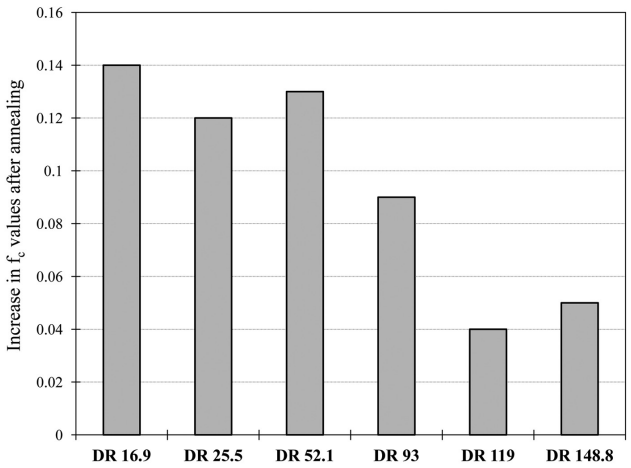

Figure 5. Observed increase in the f_c values after annealing for different draw ratios.

values, it is noticed that at low draw ratios, the lamellae were not well-aligned perpendicular to the flow direction; nevertheless, at high draw ratios the lamellae aligned themselves perpendicular to the machine direction, resulting in higher orientation.

The amorphous phase orientation, f_{am}, obtained from the absorbance band at 1368 cm^{-1} is very small (close to 0) for the lower draw ratios and its value slightly increased (close to 0.1) for the higher draw ratios. The f_{am} values for the annealed films are also in the same range, and it is seen that annealing treatment has a negligible influence on amorphous phase orientation.

From the orientation functions values in Table 3 for the annealed films it is found that both the f_a and f_b values tend to decrease after annealing. Consequently, annealing results in an increase in the *c*-axis orientation function, f_c, for all draw ratios. As annealing is performed, it is suggested that during annealing, the lamellae orient perpendicular to the machine direction. Also, melting of small lamellae and their recrystallization with better orientation can occur.

In row nucleated lamellar morphologies, lamellae can be twisted only if both *a*- and *c*-axes preferentially orient to MD [11]. Therefore, the observed decrease in the f_a values and the consequent increase in the f_c values after annealing, demonstrates that annealing can reduce the amount of twisted lamellae in HDPE cast films, in other words, annealing procedure is observed to promote parallel planar lamellae textures.

To evaluate the effectiveness of the annealing treatment on enhancement of crystalline orientation, the observed increase in the f_c values after annealing for the cast films with different draw ratios was calculated and the results are given in Figure 5. It is evident that the increase in the f_c values after annealing is much higher for the samples with lower draw ratios, and this increase is lower for the films with higher draw ratios, i.e. DR 119 and DR 148.8. Therefore, utilizing annealing treatment to improve the crystalline orientation is observed to be more effective for the films with lower draw ratios.

CONCLUSION

The influence of applying a wide range of draw ratios as well as annealing treatment on the crsytalline structure of HDPE cast films were investigated. In the cast film extrusion process although the most important processing parameter which affects the row-nucleated lamellar structures and orientation state of crystalline phase, is the value of applied draw ratios; however, annealing of the cast films improves the orientation of the crystalline phase companied with the removing of the defects in the crystalline structure and induces the perfecting of crystals. In addition, the analysis of orientation functions of crystalline phase axes suggests that annealing can reduce the twisted lamellar structures since it increases the f_c values and decreases the f_a values simultaneously. It was also seen that annealing treatment negligibly influenced amorphous phase orientation. Furthermore, it was found that effect of annealing on crystal orientation evolution (increase in *c*-axis orientation function, f_c) is more prominent for the films with lower draw ratios.

ACKNOWLEDGEMENTS

The authors gratefully thank Dr. HesamTabatabaei (École Polytechnique de Montréal) and Dr. Mikhail Malanin (IPF-Dresden) for their helpful comments and discussions. Thanks also go to Dr. Christina Scheffler and Mrs. Sabine Krause for DSC measurements, and Mrs. Regine Boldt and Mrs. Maria Auf der Landwehr for SEM imaging at IPF-Dresden.

REFERENCES

1. Nogales A, Hsiao BS, Somani RH, Srinivas S, Tsou AH, Balta-Calleja FJ, Ezquerra TA (2001) Shear-induced crystallization of isotactic polypropylene with different molecular weight

distributions: In situ small-and wide-angle X-ray scattering studies. Polymer 42: 5247-5256
2. Sadeghi F, Ajji A, Carreau P (2005) Study of polypropylene morphology obtained from blown and cast film processes: Initial morphology requirements for making membranes porous by stretching. J Plast Film Sheet 21: 199-216
3. Tabatabaei SH, Carreau PJ, Ajji A (2009) Effect of processing on the crystalline orientation, morphology, and mechanical properties of polypropylene cast films and microporous membrane formation. Polymer 50: 4228-4240
4. Seki M, Thurman DW, Oberhauser JP, Kornfield JA (2002) Shear-mediated crystallization of isotactic polypropylene: The role of long chain-long chain overlap. Macromolecules 35: 2583-2594
5. Bafna A, McFaddin D, Beaucage G, Merrick-Mack J, Mirabella FM (2007) Integrated mechanism for the morphological structure development in HDPE melt-blown and machine-direction-oriented films. J Polym Sci B: Polym Phys 45: 1834-1844
6. Prasad A, Shroff R, Rane S, Beaucage G (2001) Morphological study of HDPE blown films by SAXS, SEM and TEM: A relationship between the melt elasticity parameter and lamellae orientation. Polymer 42: 3103-3113
7. Lee S-Y, Park S-Y, Song H-S (2007) Effects of melt-extension and annealing on row-nucleated lamellar crystalline structure of HDPE films. J Appl Polym Sci 103: 3326-3333
8. Hu B, Lei C, Xu R, Shi W, Cai Q, Mo H, Chen C (2013) Influence of melt-draw ratio on the structure and properties of poly (vinylidiene fluoride) cast film. J Plast Film Sheet 30: 300-313
9. Sadeghi F, Ajji A, Carreau PJ (2007) Analysis of row nucleated lamellar morphology of polypropylene obtained from the cast film process: Effect of melt rheology and process conditions. Polym Eng Sci 47: 1170-1178
10. Yu T-H,Wilkes GL (1996) Orientation determination and morphological study of high density polyethylene (HDPE) extruded tubular films: Effect of processing variables and molecular weight distribution. Polymer 37: 4675-4687
11. Zhang X, Elkoun S, Ajji A, Huneault M (2004) Oriented structure and anisotropy properties of polymer blown films: HDPE, LLDPE and LDPE. Polymer 45: 217-229
12. Schrauwen B, Breemen Lv, Spoelstra A, Govaert L, Peters G, Meijer H (2004) Structure, deformation, and failure of flow-oriented semicrystalline polymers. Macromolecules 37: 8618-8633
13. Hedesiu C, Demco DE, Kleppinger R, Buda AA, Blümich B, Remerie K, Litvinov VM (2007) The effect of temperature and annealing on the phase composition, molecular mobility and the thickness of domains in high-density polyethylene. Polymer 48: 763-777
14. Hedesiu C, Demco D, Kleppinger R, Poel GV, Gijsbers W, Blümich B, Remerie K, Litvinov V (2007) Effect of temperature and annealing on the phase composition, molecular mobility, and the thickness of domains in isotactic polypropylene studied by proton solid-state NMR, SAXS, and DSC. Macromolecules 40: 3977-3989
15. Bai H, Luo F, Zhou T, Deng H, Wang K, Fu Q (2011) New insight on the annealing induced microstructural changes and their roles in the toughening of β-form polypropylene. Polymer 52: 2351-2360
16. Johnson MB, Wilkes GL (2002) Microporous membranes of isotactic poly (4-methyl-1-pentene) from a melt-extrusion process. II. Effects of thermal annealing and stretching on porosity. J Appl Polym Sci 84: 1076-1100
17. Johnson MB, Wilkes GL (2002) Microporous membranes of polyoxymethylene from a melt-extrusion process:(II) Effects of thermal annealing and stretching on porosity. J Appl Polym Sci 84: 1762-1780
18. Humbert S, Lame O, Séguéla R, Vigier G (2011) A re-examination of the elastic modulus dependence on crystallinity in semi-crystalline polymers. Polymer 52: 4899-4909
19. Ding Z, Bao R, Zhao B, Yan J, Liu Z, Yang M (2013) Effects of annealing on structure and deformation mechanism of isotactic polypropylene film with row-nucleated lamellar structure. J Appl Polym Sci 130: 1659-1666
20. Saffar A, Ajji A, Carreau PJ, Kamal MR (2014) The impact of new crystalline lamellae formation during annealing on the properties of polypropylene based films and membranes. Polymer 55: 3156-3167

21. Bai H, Wang Y, Zhang Z, Han L, Li Y, Liu L, Zhou Z, Men Y (2009) Influence of annealing on microstructure and mechanical properties of isotactic polypropylene with β-phase nucleating agent. Macromolecules 42: 6647-6655
22. Offord GT, Armstrong SR, Freeman BD, Baer E, Hiltner A, Swinnea JS, Paul DR (2013) Porosity enhancement in β nucleated isotactic polypropylene stretched films by thermal annealing. Polymer 54: 2577-2589
23. Peacock A (2000). Handbook of polyethylene: Structures: Properties, and applications, Marcel Dekker, Inc.
24. Kebritchi A, Nekoomansh M, Mohammadi F, Khonakdar HA (2014) The role of 1-hexene comonomer content in thermal behavior of medium density polyethylene (MDPE) synthesized using Phillips catalyst. Polyolefins J 1: 117-129
25. Lee S-Y, Park S-Y, Song H-S (2006) Lamellar crystalline structure of hard elastic HDPE films and its influence on microporous membrane formation. Polymer 47: 3540-3547
26. Chatterjee T, Patel R, Garnett J, Paradkar R, Ge S, Liu L, Forziati KT, Shah N (2014) Machine direction orientation of high density polyethylene (HDPE): Barrier and optical properties. Polymer 55: 4102-4115
27. Siesler H (1984) Rheo-optical Fourier-Transform Infrared Spectroscopy (FTIRS) of polymers-6: Changes of crystal-axes orientation and state of order during uniaxial elongation of high-density polyethylene. Infrared Phys. 24: 239-244
28. Siesler H (1984) Rheo-optical Fourier-Transform infrared spectroscopy: Vibrational spectra and mechanical properties of polymers. Adv Polym Sci 65: 1-77
29. Tabatabaei SH, Carreau PJ, Ajji A (2008) Microporous membranes obtained from polypropylene blend films by stretching. J Membr Sci 325: 772-782
30. Wunderlich B (1973) Macromolecular Physics, Volume 1: Crystal structure, morphology, defects, Academic Press.
31. Schultz J, Hsiao BS, Samon J (2000) Structural development during the early stages of polymer melt spinning by in-situ synchrotron X-ray techniques. Polymer 41: 8887-8895
32. Samon JM, Schultz JM, Hsiao BS (2002) Structure development in the early stages of crystallization during melt spinning. Polymer 43: 1873-1875